PURDUE UNIVERSITY
SCHOOL OF AERONAUTICS AND ASTRONAUTICS

(NASA-CR-181197) MULTI-INPUT MULTI-OUTPUT SYSTEM CONTROL FOR EXPERIMENTAL AIRCRAFT Final Technical Report (Purdue Univ.) 58 p
Avail: NTIS HC A04/MF A01 CSCL 01C

N87-26915

Unclas
G3/08 0087891

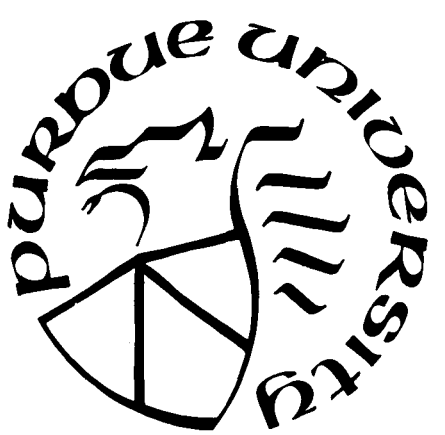

West Lafayette, Indiana 47907

FINAL TECHNICAL REPORT

ON

MULTI-INPUT MULTI-OUTPUT SYSTEM CONTROL FOR EXPERIMENTAL AIRCRAFT

NCC2-288

August 20, 1987

Principal Investigator: David K. Schmidt
School of Aeronautics and Astronautics
Purdue University
West Lafayette, IN 47907

Technical Monitor: Mr. E.L. Duke
Mr. Frank Jones
NASA Ames/Dryden Flight Research Facility
P.O. Box 273
Edwards, CA 93523

Preface

The report attached as Appendix A documents the research performed by the School of Aeronautics and Astronautics, Purdue University, for the NASA Ames Research Center/Dryden Flight Research Facility, under Cooperative Agreement/Grant Number NCC2-288*. The objective of the program was to determine the applicability of several multi-input/multi-output control synthesis techniques for the synthesis of flight control laws for advanced experimental aircraft, and to extend the techniques as necessary to obtain simple, robust control laws that meet specific handling qualities objectives.

This report includes results from the synthesis of control laws for an advanced STOL vehicle in a low-speed approach flight condition. Two of four candidate synthesis techniques are reported herein - direct eigenspace assignment and explicit model following via a Linear Quadratic Regulator (LQR) formulation. The other two techniques under current investigation, but *not* considered as part of this grant activity, are implicit model following (also via LQR) and Cooperative Control Synthesis. This latter technique has been a topic of continued research at Purdue University, and utilizes pilot-in-the-loop (pilot modeling) techniques.

A fundamental objective in this work was to obtain low-order feedback compensators, synthesized via the techniques above, and judicious use of state-estimation thus allowing the use of a reasonable number of sensors for feedback. Although this report focuses on the results from the synthesis of state-feedback control laws, two state-estimation techniques under consideration are also noted. In implementing these estimation techniques, we are interested in the ultimate stability robustness of the system, and not increasing the dynamic order of the stick-response transfer functions. The latter goal is motivated by the desire to preserve the handling characteristics "built into" the state-feedback control law utilized.

---

* Mr. E.L. Duke, Technical Monitor

Appendix A -

Multi-input Multi-output Control Law Synthesis For Experimental Aircraft

Contents

1. INTRODUCTION

The ultimate performance objective of the flight control design is to make the combined pilot and vehicle system behave suitably. This objective introduces the idea of "handling qualitities", defined as those desirable dynamic traits of an aircraft that will help the pilot and vehicle system perform their intended mission. With the "handling qualities" specifications available to the control system designer, he must use these specifications to formulate and implement the control system design, and finally to verify that the augmented vehicle does indeed meet the handling qualities specifications.

In the past decade or so, many new methodologies for designing control systems for multi-input multi-output systems have emerged. The objective of this study is to investigate the applicability of some of these 'modern' techniques to design of flight control systems, with the specific objective of meeting the handling qualities reqirements.

In this particular study, two of these techniques - direct eigenspace assignment (DEA) and explicit model following (EMF), are used initially to synthesize control laws for the logitudinal dynamics model of a STOL vehicle in the landing approach configuration. The vehicle model and the flight control design requirements are presented in Section 2. In the succeeding sections, the two synthesis techniques are briefly discussed and the handling qualities specifications mapped into the algorithm formulation. The control laws resulting from exercising the algorithms are evaluated in terms of achieved performance and robustness.

Since the synthesized control laws involve full-state feedback, methodologies for implementing these control laws using output feedback, and without adversely affecting performance and robustness, are a topic of significant interest and are presently being pursued. Promising techniques being considered are briefly discussed in Section 5.

Finally, the salient features of the two design techniques are summarized and the areas that require further investigation are suggested.

2. THE STUDY VEHICLE

2.1 Vehicle Model Description

The vehicle considered is a STOL aircraft, with an airframe similar to an F-18 aircraft. The linearized dynamic model for the longitudinal axis includes four rigid-body degrees of freedom and three first order actuator lags (each at 15 rads/sec). The trim values for the landing approach flight condition are listed in Table 2.1. The control inputs to be utilized are the horizontal tail (elevator), the thrust vector angle for a 2-D nozzle, and the trailing edge flap. The state vector for the vehicle model is

$$\bar{x}^T = [\bar{u}_f, \alpha, q, \theta, \delta_H, \delta_{TV}, \delta_F]$$

where

$\bar{u}_f$ = nondimensional forward speed ($\frac{u_f}{U_0}$)

α = angle of attack (rads)

q = pitch rate (rads/sec)

θ = pitch angle (rads)

δ_H = horizontal tail deflection (rads)

δ_{TV} = Thrust vector angle (rads)

δ_F = trailing edge flap deflection (rads)

with the control inputs taken as commands to the servo actuators, or

$$\bar{\delta}_c^T = [\delta_{Hc}, \delta_{TVc}, \delta_{Fc}]$$

The vehicle responses of interest are

$$\bar{y}^T = [n_z, q, \theta, \gamma, \bar{u}]$$

where

n_z = normal acceleration at C.G. (g's, +ve up)

γ = flight path angle (rads)

The vehicle dynamics can then be written in the form

$$\dot{\bar{x}} = A\bar{x} + B\bar{\delta}_c$$

$$\bar{y} = C\bar{x}$$

The open loop system matrices are listed in Table 2.2. The open-loop vehicle eigenvalues are

$$\lambda_{1,2} = 0.1557 \pm j\,0.1968\,, \quad \lambda_3 = -1.535\,, \quad \lambda_4 = 0.8532$$

Note the unstable pole.

2.2 Flight Control Design Requirements

The flight control design requirements can be summarized as follows

* Explicitly include handling quality criteria
* Avoid excessive control surface rates
* Reduce control energy at high frequencies

The handling quality criteria is stated in terms of desired short period pitch rate response and the phase relationship between the flight path angle and the pitch angle i.e.

$$\frac{q}{F_s} = \left(\frac{q}{F_s}\right)_{ss} \frac{\omega_{sp}^2 \tau_{\theta_2}\left(s + 1/\tau_{\theta_2}\right)}{\left(s^2 + 2\zeta_{sp}\omega_{sp}s + \omega_{sp}^2\right)}$$

and

$$\frac{\gamma}{\theta} = \frac{1/\tau_{\theta_2}}{\left(s + 1/\tau_{\theta_2}\right)}$$

with

$$\left(\frac{q}{F_s}\right)_{ss} = 0.5 \text{ deg/sec/lbs} \quad , \quad \tau_{\theta_2} = 0.75 \text{ secs}$$

and ω_{sp} and ζ_{sp} selected so as to satisfy Level 1 handling qualities requirement [1] and a rise time for pitch rate, t_{R_q} = 0.8 sec. Furthermore, the augmented vehicle should exhibit classical "phugoid" like dynamics for the low frequency mode.

In the present study, our primary objective will be to meet the above handling qualities specifications through proper control augmentation of the vehicle.

Table 2.1 Trim values for STOL model

U_o	202 ft/sec
θ_o	4.72°
α_o	7.72°
γ_o	-3.0°
h_o	200 ft
q	48.5 psf

Table 2.2 Open Loop System Matrices

A =

$$\begin{bmatrix} -0.0575 & -0.2023 & -0.1321 & -0.1589 & 0.0351 & -0.0085 & -0.0322 \\ -0.2900 & -0.3237 & 0.9758 & -0.0130 & -0.0910 & -0.0483 & -0.1011 \\ -0.6088 & 1.1693 & -0.6121 & 0.0061 & -1.7627 & -1.4325 & 0.2021 \\ 0. & 0. & 1.0000 & 0. & 0. & 0. & 0. \\ 0. & 0. & 0. & 0. & -15.0000 & 0. & 0. \\ 0. & 0. & 0. & 0. & 0. & -15.0000 & 0. \\ 0. & 0. & 0. & 0. & 0. & 0. & -15.0000 \end{bmatrix}$$

B =

$$\begin{bmatrix} 0. & 0. & 0. \\ 0. & 0. & 0. \\ 0. & 0. & 0. \\ 0. & 0. & 0. \\ 15. & 0. & 0. \\ 0. & 15. & 0. \\ 0. & 0. & 15. \end{bmatrix}$$

C =

$$\begin{bmatrix} 1.8382 & 2.0402 & 0.1089 & 0. & 0.5730 & 0.2865 & 0.6303 \\ 0. & 0. & 1.0000 & 0. & 0. & 0. & 0. \\ 0. & 0. & 0. & 1.0000 & 0. & 0. & 0. \\ 0. & -1.0012 & 0. & 1.0000 & 0. & 0. & 0. \\ 1.0000 & 0. & 0. & 0. & 0. & 0. & 0. \end{bmatrix}$$

3. DIRECT EIGENSPACE ASSIGNMENT (DEA)

3.1 Gain Synthesis

In the direct eigenspace assignment technique, the control objectives are stated in terms of a desired eigenstructure for the augmented system. For the state feedback case, the synthesis problem is as follows

Given a system

$$\dot{\bar{x}} = A\bar{x} + B\bar{u}, \; x \in R^n \qquad \text{(system dynamics)}$$

$$\bar{u} = \bar{u}_c + \bar{u}_p \;, \; \bar{u} \in R^m \qquad \text{(total control input)}$$

$\bar{u}_p$ = pilot's control inputs

$$y = C\bar{x} \;, \; \bar{y} \in R^p \qquad \text{(system responses)}$$

find a control law of the form

$$\bar{u}_c = -K\bar{x}$$

to achieve some desired eigenspace for the augmented system

$$\dot{\bar{x}} = (A - BK)\bar{x} + B\bar{u}_p$$

$$y = C\bar{x}$$

To determine K, note that the augmented (closed-loop) system eigenvalues and eigenvectors are related by

$$(A - BK)\,\bar{v}_{c_i} = \lambda_{c_i}\,\bar{v}_{c_i} \qquad i = 1, \ldots n \qquad (3.1.1)$$

where

λ_{c_i} = closed-loop eigenvalue

$\bar{v}_{c_i}$ = closed-loop eigenvector

For full-state feedback, the limitation on the achievable eigen-

space is that all the desired closed-loop eigenvalues can be exactly placed while only "m" elements of their associated eigenvectors may be specified (where m = dimension of $\bar{u}$). Since in general $m < n$, we cannot exactly obtain all elements of the desired eigenvector for each closed-loop mode. One approach is to determine the "best" achievable eigenvector $\bar{v}_{a_i}$, for each of the closed-loop modes, that minimizes the mode's cost function

$$J_i = \frac{1}{2}\left(\bar{v}_{a_i} - \bar{v}_{d_i}\right)^* Q_{d_i}\left(\bar{v}_{a_i} - \bar{v}_{d_i}\right) \qquad i=1,\ldots,n \qquad (3.1.2)$$

where

$\bar{v}_{a_i}$ = i'th achievable eigenvector associated with eigenvalue

$\bar{v}_{d_i}$ = i'th desired eigenvector

Q_{d_i} = i'th n-by-n symmetric positive semi-definite weighting matrix on eigenvector error elements

and * denotes conjugate transpose.

Equation (3.1.1) can be rewritten as

$$\left(\lambda_i I - A\right)\bar{v}_{a_i} = -BK\,\bar{v}_{a_i} \qquad (3.1.3)$$

Defining the vector $\bar{w}_i \triangleq -K\bar{v}_{a_i}$ and using eqn. (3.1.3), the solution to (3.1.2) is obtained as

$$\bar{w}_i^* = v_{d_i}^* Q_{d_i} L_i \left[L_i^* Q_{d_i} L_i\right]^{-1}$$

where $L_i = (\lambda_i I - A)^{-1} B$.

Once $\bar{w}_i$ are obtained, the achievable eigenvectors are given by

$$\bar{v}_{a_i} = L_i\,\bar{w}_i \qquad i=1,\ldots,n$$

and the feedback gains are obtained as

$$K = -WV^{-1}$$

where

$$W = [\bar{w}_1 \quad \bar{w}_2 \quad \ldots \quad \bar{w}_n]$$

and

$$V = [\bar{v}_{a_1} \quad \bar{v}_{a_2} \quad \ldots \quad \bar{v}_{a_n}]$$

This solution algorithm is due to Schmidt and Davidson [2]. A macro using MATRIX$_X$ commands was written to implement the above synthesis procedure. This macro is documented in the Appendix. The block diagram for DEA control law implementation is shown in Fig. 3.1.

3.2 Selection of Desired Eigenspace and Resulting Control Law

The control design objective is to make the augmented vehicle modes like those of a "classical" airplane i.e. the phugoid and short period modes. For this initial synthesis, we chose the desired phugoid mode to be

$$\omega_{ph} = 0.25 \text{ rads/sec} \quad , \quad \zeta_{ph} = 0.1$$

$$\Rightarrow \lambda_{ph} = -0.05 \pm j\,0.2487$$

with the corresponding desired eigenvector selected as

$$\bar{v}_{d_{ph}}^T = [1 \pm ja, \; 0, \; a, \; a \pm j1, \; a, \; a, \; a] \quad \text{(note state def., pg. 3)}$$

where "a" denotes an arbitrary value. The above choice for the phugoid eigenvector reflects the desire that the phugoid mode shape be dominated by forward speed and pitch attitude response with little or no angle of attack contribution [4].

The short-period mode frequency and damping are selected to reflect the handling qualities requirements. This choice is as follows

$$\omega_{sp} = 3.7 \text{ rads/sec} \quad , \quad \zeta_{sp} = 0.75$$

$$\Rightarrow \lambda_{sp} = -2.78 \pm j\,2.43$$

The choice of the desired short-period eigenvector is based on the requirement that the short-period mode be dominant in angle of attack

and pitch rate response, with little or no forward speed contribution. Furthermore, the short-period eigenvector should reflect the desired flight path angle to pitch attitude phase relationship i.e. we want

$$\left.\frac{\gamma}{\theta}\right|_{sp} \hat{=} \frac{1/\tau_{\theta_2}}{(s+1/\tau_{\theta_2})}$$

Using the relationship $\gamma = \theta - \alpha$, we can write the above constraint as

$$\left.\frac{\alpha}{q}\right|_{sp} \hat{=} \left.\frac{1}{(s+1/\tau_{\theta_2})}\right|_{s=\lambda_{sp}}$$

With $\tau_{\theta_2} = 0.75$ sec and $\lambda_{sp} = -2.78 \pm j\,2.43$, we get the desired relationship between

α and q in the short-period mode to be

$$\left.\frac{\alpha}{q}\right|_{sp} = -0.181 \mp j\,0.3038$$

Then an eigenvector that results is

$$\bar{v}_{d_{sp}}^{T} = [0, -0.181 \mp j\,0.3038, 1, a, a, a, a] \quad \text{(note state def., pg.3)}$$

The above choice as well as the desired eigenspace for the actuator modes is listed in Table 3.1. The actuator poles are left near their open loop values, and the corresponding eigenvectors are selected simply to obtain decoupled actuator modes.

From Table 3.1 we note that for the short period mode and for all the three actuator modes, we are in effect specifying only three elements of the corresponding eigenvectors. Since we have three controls available, we shall be able to exactly achieve the specified elements of these eigenvectors. The phugoid eigenvector effectively has only two specified elements. This leaves one extra degree of freedom to further constrain the phugoid eigenvector. One possibility to be explored in the future is to use this freedom to reduce the control surface deflections.

The achieved eigenvectors corresponding to the above selections are listed in Table 3.2, and the associated feedback control gains in Table 3.3. As we expected, the desired eigenspace is achieved exactly. For comparison, the phasor diagrams for the open-loop and achievable eigenvectors are shown in Fig. 3.2. These indicate "classical" phugoid and short-period mode like behaviour for the augmented airplane. Note, however, the large control deflections in these mode shapes, indicating high deflection requirements for this control law.

3.4 Performance Evaluation

With the pilot's input taken to be commanded horizontal tail deflection ($\delta_{H_{P_C}}$), the transfer functions between the responses of interest and the pilot's input are listed in Table 3.4. These transfer functions indicate that the augmented system response exhibits the desired decoupling between the phugoid and the short period mode. Moreover, q/α when calculated from these transfer functions for $s = \gamma_{sp}$ does give the value ($-0.181 \mp j0.3038$) that was specified during the design process. Also in the $q/\delta_{H_{P_C}}$ transfer function, note that $1/\tau_{\theta_2}$ has increasd to 0.92 from its open loop value of 0.5 sec^{-1}.

Other responses of interest are the normal acceleration at the center of rotation ($n_{z_{CR}}$) and the flight path angle at the center of rotation (γ_{CR}). With the horizontal tail deflection as the only pilot input, the center of rotation is located 10.45 ft ahead of the C.G. The transfer functions for these responses are also listed in Table 3.4

The transfer functions from pilot's control input to the actual control deflections are listed in Table 3.5.

Time histories for a step pilot input ($\delta_{H_{P_C}} = 1^\circ$) are shown in Figs.

3.3 to 3.5. Fig. 3.3 shows the response for the augmented vehicle states - these again indicate the decoupled phugoid and short-period mode behaviour. Fig. 3.4 shows the response for normal acceleration and flight path angle, both at the C.G. as well as the center of rotation. Fig. 3.5 shows the actual control deflections for this step pilot input.

3.5 Robustness Evaluation

A very important consideration in flight control design is the stability robustness of the augmented system. Given a system with transfer function matrix G(s), where

$$G(s) = [sI - A]^{-1} B$$

a reliable (but sometimes conservative [5]) measure of robustness is the minimum singular value of the return difference matrix, evaluated as a function of $j\omega$, or in this case, with the loop broken at the input,

$$\underline{\sigma}[I + KG(s)]$$

For the control law obtained above, the singular values of the return difference matrix are plotted in Fig. 3.6. Note the relatively low stability margins in the frequency range of upto 4 rads/sec (the frequency range of the vehicle, except for the actuators). How to increase this robustness requires additional consideration.

A more "classical" approach to evaluating the stability robustness is to "break" one loop at a time (i.e. one loop open and the other loops closed). The eigenvalues of the system with the various loops open, and for the above control law, are listed in Table 3.6. (Note that the system with δ_H loop open has one unstable pole, which means that the control law will not be able to stabilize the vehicle in case of an elevator actuator failure). The Bode plots for the one-loop-at-a-time

analysis are shown in Figs. 3.7(a)-(c). These plots appear to indicate "good" gain and phase margins in all the three control loops. This might be optimistic in light of the stability margins based on the singular value analysis. Whether this controller has sufficient robustness is an open question. If not, how to improve robustness is a topic of interest.

Table 3.1 Desired Eigenspace

$$\bar{x}^T = [\bar{u}_f, \alpha, q, \theta, \delta_H, \delta_{TV}, \delta_F]$$

Phugoid	Short Period	δ_H Actuator	δ_{TV} Actuator	δ_F Actuator
(-.05±j0.2487)	(-2.78±j2.43)	(-14.9)	(-15.1)	(-15.2)
1. ±ja	0.	a	a	a
0.	-0.1809∓j0.3038i	a	a	a
0.	1.	a	a	a
a ±j1.	a	a	a	a
a	a	1.	0.	0.
a	a	0.	1.	0.
a	a	0.	0.	1.

(a denotes arbitrary)

Table 3.2 Achieved Eigenspace

$$\bar{x}^T = [\bar{u}_f, \alpha, q, \theta, \delta_H, \delta_{TV}, \delta_F]$$

Phugoid	Short Period	δ_H Actuator	δ_{TV} Actuator	δ_F Actuator
(−.05±j0.2487)	(−2.78±j2.43)	(−14.9)	(−15.1)	(−15.2)
1.2504∓j4.4973	0.	−0.0014	0.0013	0.0021
−0.0105∓j0.0907	−0.1809∓j0.3038	−0.0021	−0.0033	0.0078
0.1621∓j1.7981	1.	0.1235	0.0992	−0.0144
−7.0750±j0.7707	−0.2039∓j0.1782	−0.0083	−0.0066	0.0009
−0.2076∓j0.1107	−0.1588∓j3.0981	1.	0.	0.
−0.7948±j1.9342	1.2138±j1.7199	0.	1.	0.
−0.7394∓j5.1039	−2.4555∓j1.0433	0.	0.	1.

Table 3.3 Feedback gains for DEA design

$$\bar{x}^T = [\bar{u}_f, \alpha, q, \theta, \delta_H, \delta_{TV}, \delta_F]$$

K =

$$\begin{bmatrix} 1.1282 & -10.1167 & -2.2662 & 0.1001 & 0.2547 & 0.1909 & 0.0437 \\ 0.2822 & 5.5829 & 0.1742 & -0.0671 & -0.0102 & 0.0068 & -0.0415 \\ -1.8886 & -2.9672 & 1.5389 & -0.3687 & -0.2018 & -0.1623 & 0.0629 \end{bmatrix}$$

Table 3.4 Transfer Functions for DEA design

$$\Delta = (s + 0.05 \pm j\,0.2487)(s + 2.78 \pm j\,2.43)$$

$$\frac{\bar{u}_\beta}{\delta_{H_{Pc}}} = \frac{0.0353\,(s + 0.551)}{(s + 0.05 \pm j\,0.2487)} \left(\frac{14.9}{s + 14.9}\right) \quad ; \quad \frac{\alpha}{\delta_{H_{Pc}}} = \frac{-0.0916\,(s + 23.93)}{(s + 2.78 \pm j\,2.43)} \left(\frac{14.9}{s + 14.9}\right)$$

$$\frac{q_V}{\delta_{H_{Pc}}} = \frac{-1.7745\,(s + 0.919)(s + 0.0739)\,s}{\Delta} \left(\frac{14.9}{s + 14.9}\right) \quad ; \quad \theta = \frac{q_V}{s}$$

$$\frac{n_z}{\delta_{H_{Pc}}} = \frac{0.577\,(s + 6.905)(s - 2.392)(s - 0.0288)(s + 0.00478)}{\Delta} \left(\frac{14.9}{s + 14.9}\right)$$

$$\frac{r}{\delta_{H_{Pc}}} = \frac{0.0917\,(s + 6.853)(s - 2.427)(s - 0.00926)}{\Delta} \left(\frac{14.9}{s + 14.9}\right)$$

$$l_{CR} = 10.45\ \text{ft} \quad ; \quad \frac{n_{z_{CR}}}{\delta_{H_{Pc}}} = \frac{2.0895\,(s - 4.7)(s - 0.0288)(s + 0.00478)}{\Delta} \left(\frac{14.9}{s + 14.9}\right)$$

$$\frac{r_{CR}}{\delta_{H_{Pc}}} = \frac{0.3182\,(s - 4.85)(s - 0.00926)}{\Delta} \left(\frac{14.9}{s + 14.9}\right)$$

Table 3.5 Control deflection Transfer functions for DEA design

$$\Delta = (s+0.05 \pm j\,0.2487)(s+2.78 \pm j\,2.43)$$

$$\frac{\delta_H}{\delta_{H_{Pc}}} = \frac{(s-2.615)(s+4.25)}{(s+2.78 \pm j\,2.43)} \left(\frac{15}{s+14.9}\right)$$

$$\frac{\delta_{TV}}{\delta_{H_{Pc}}} = \frac{0.1527\,(s+0.037 \pm j\,0.2323)(s+78.13)}{\Delta} \left(\frac{15}{s+15.1}\right)$$

$$\frac{\delta_F}{\delta_{H_{Pc}}} = \frac{3.027\,(s-0.0577)(s+0.0717)(s-1.364)}{\Delta} \left(\frac{15}{s+15.2}\right)$$

Table 3.6 Eigenvalues for one-loop-at-a-time analysis

δ_H loop open, λ = $-0.0516 \pm j0.247$, 2.615, -4.2508, -15, -15.1, -15.2

δ_{TV} loop open, λ = $-0.0494 \pm j.2374$, $-2.7796 \pm j3.8517$, -14.9, -15, -15.2

δ_F loop open, λ = $-0.0421 \pm j.2088$, $-2.416 \pm j2.251$, -14.9, -15, -15.1

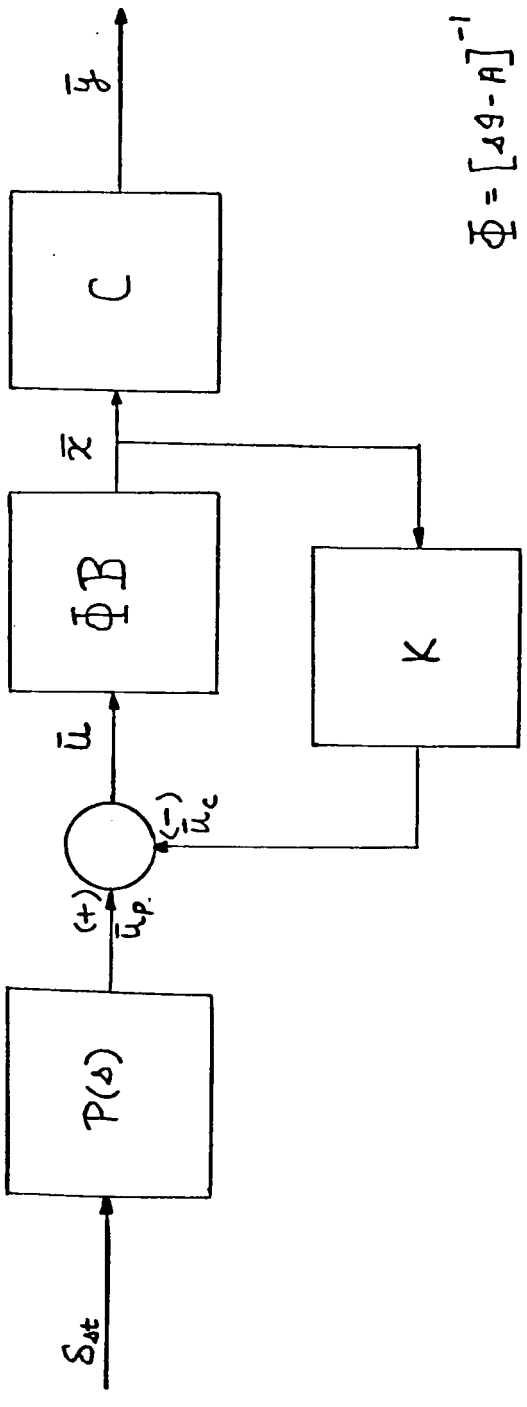

Figure 3.1 DEA Control Law Implementation

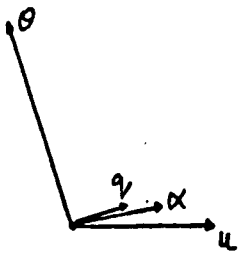

$\lambda_{1,2} = -0.1557 \pm j\,0.1967$

$\lambda_4 = 0.8531$

$\lambda_3 = -1.535$

(a) Open Loop

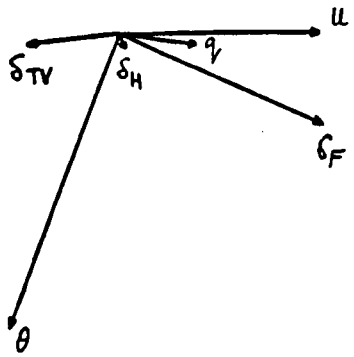

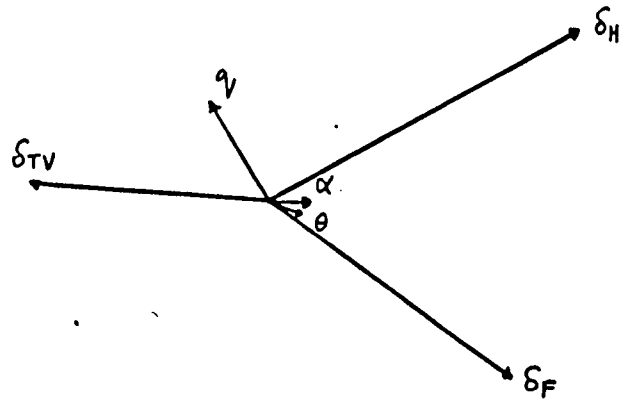

(b) Augmented System

$\lambda_{MR} = -0.05 + j\,0.2487$

$\lambda_4 = -2.78 + j\,2.43$

Figure 3.2 Eigenvector Phasor Diagrams

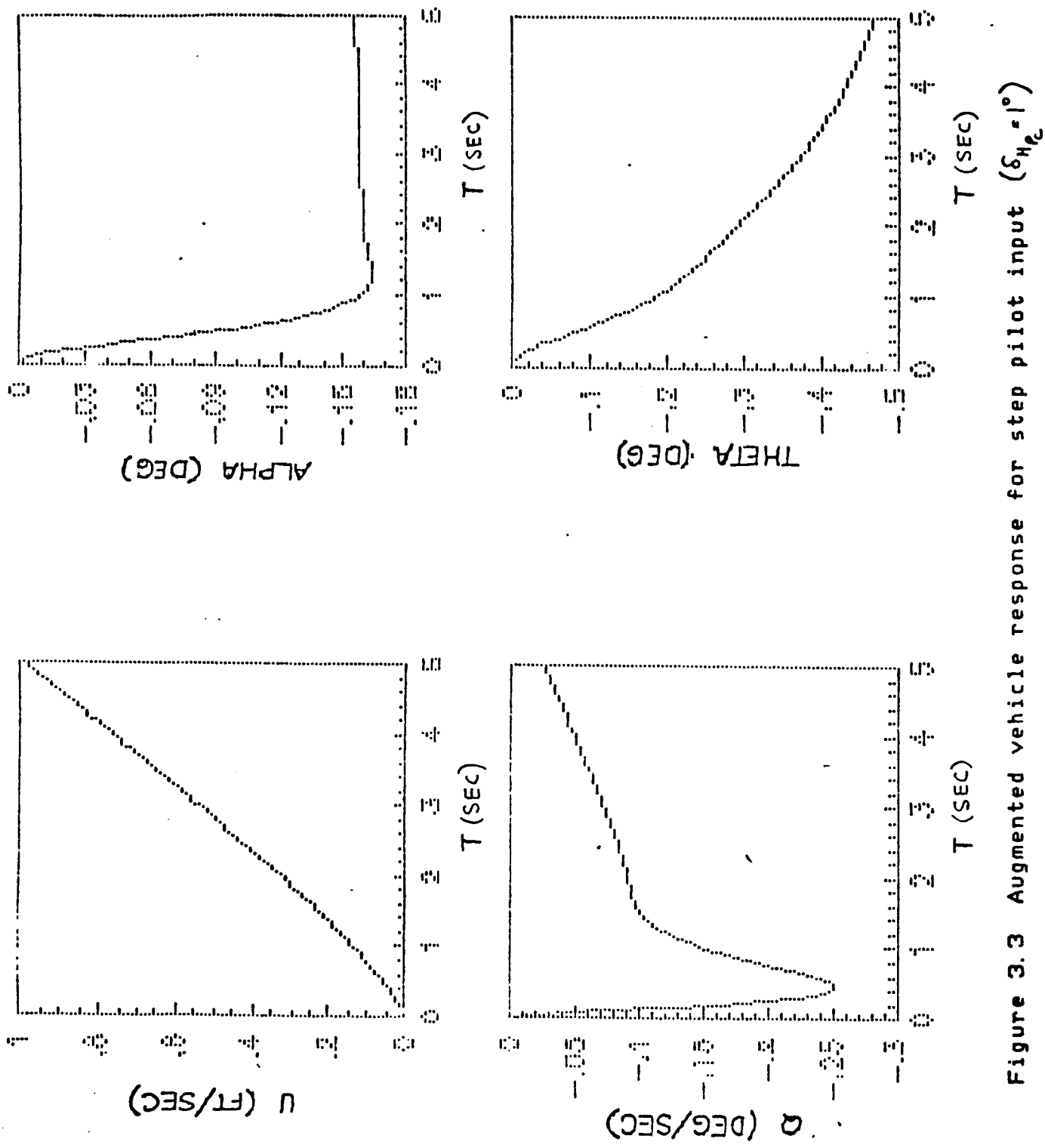

Figure 3.3 Augmented vehicle response for step pilot input ($\delta_{H_{PC}} = 1°$)

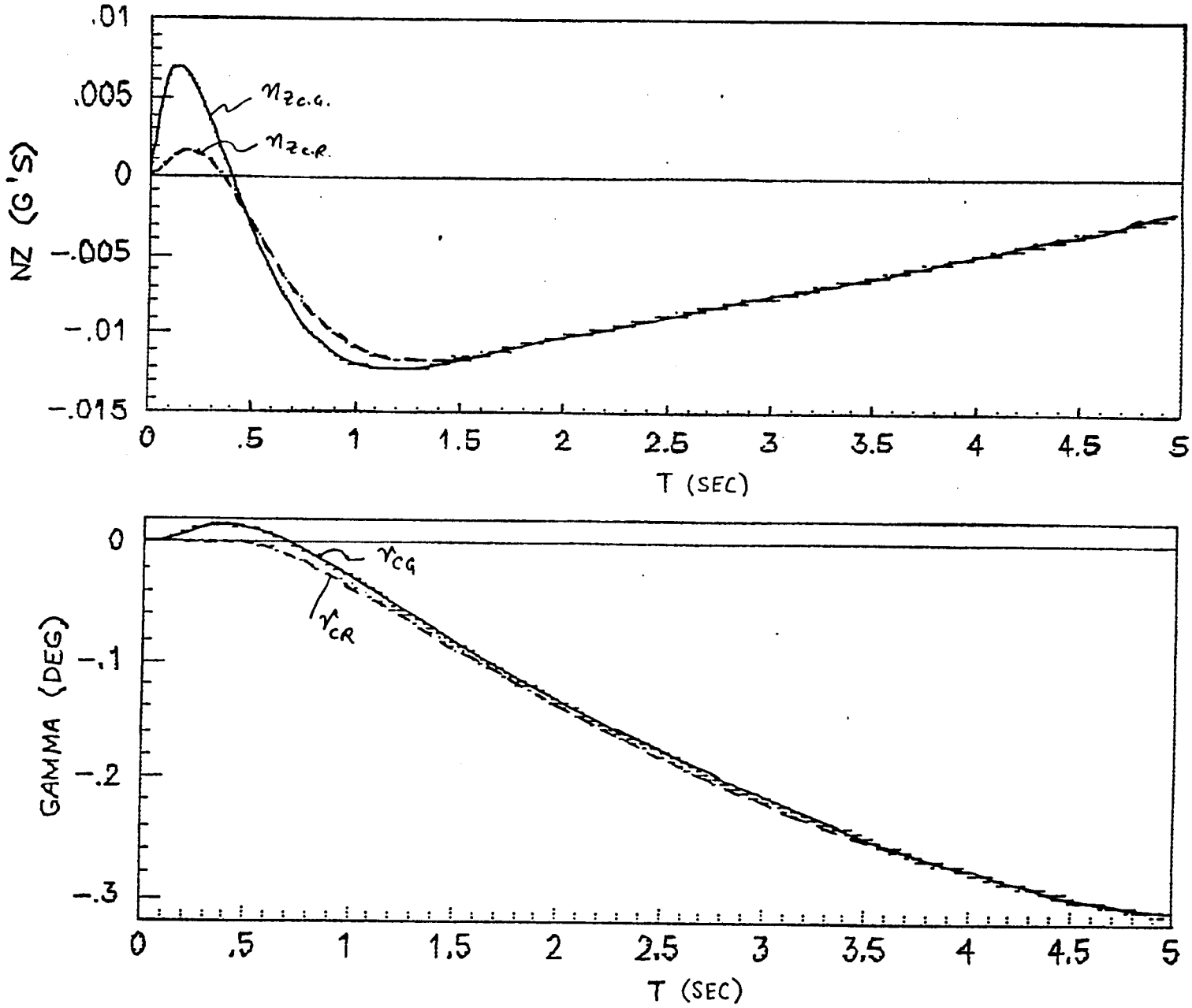

Figure 3.4 n_z and γ response for step pilot input ($\delta_{H_{Pc}} = 1°$)

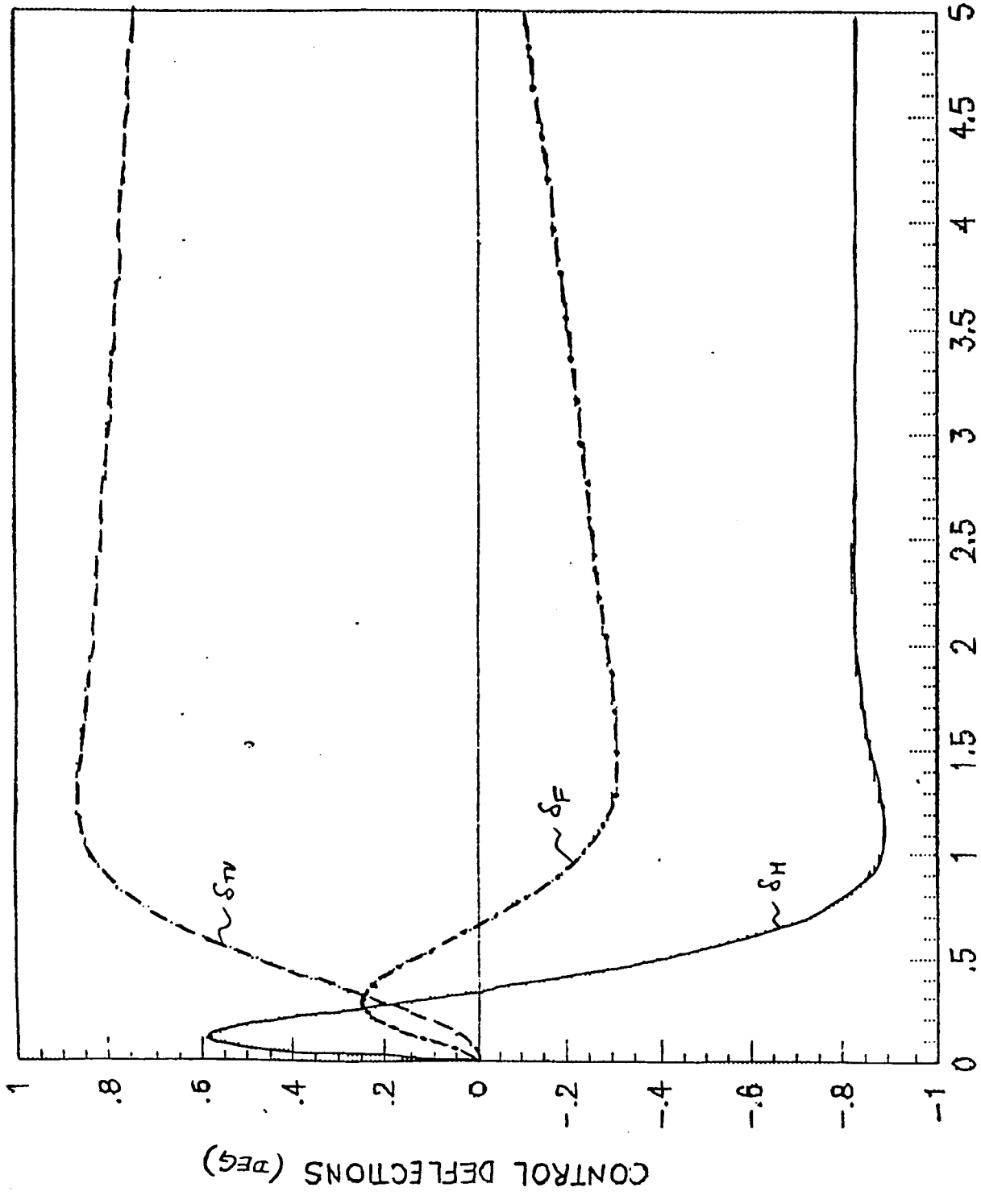

Figure 3.5 Control Deflections for step pilot input ($\delta_{H_{PC}}=1°$)

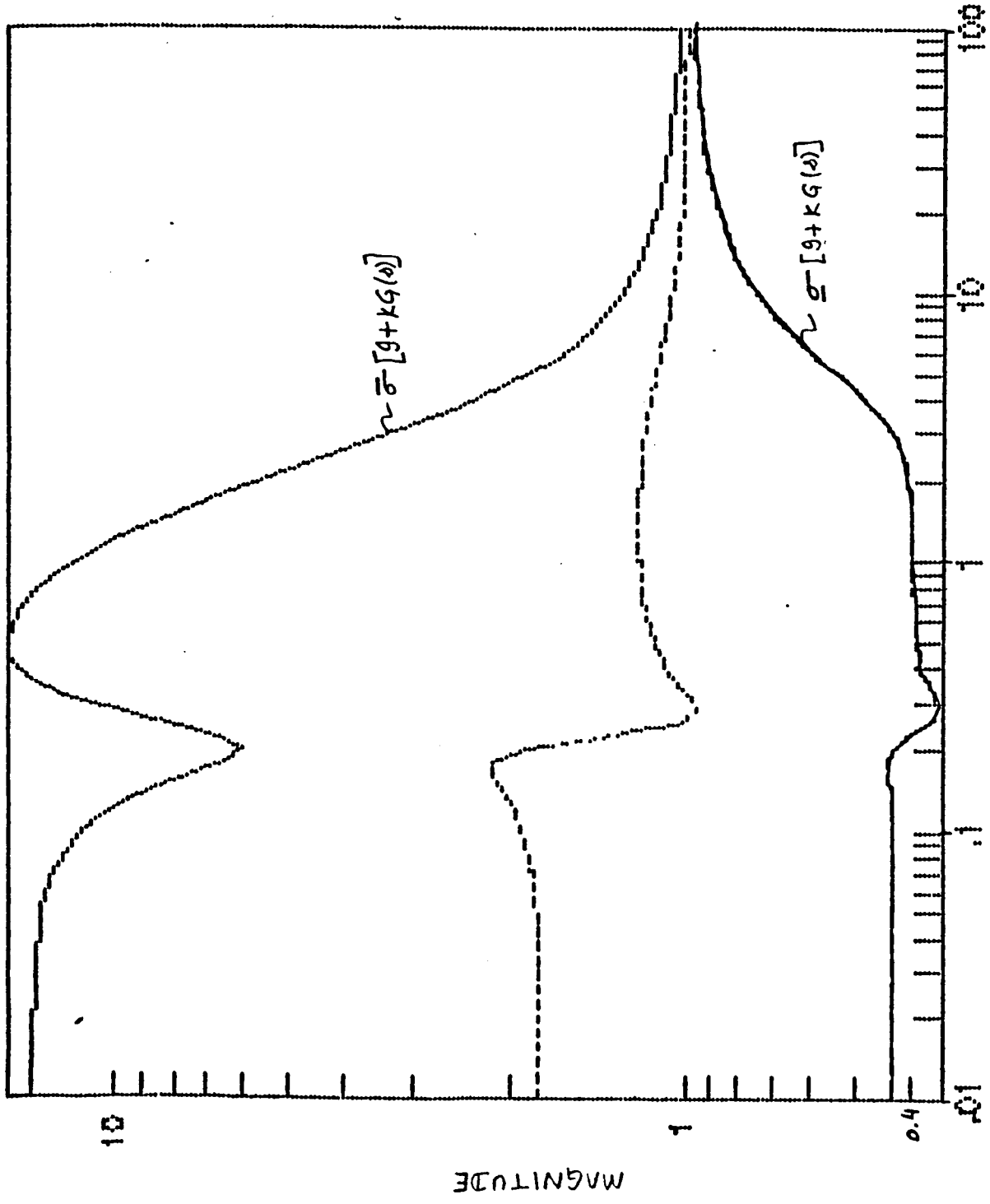

Figure 3.6 Singular values of return difference matrix at input (DEA design)

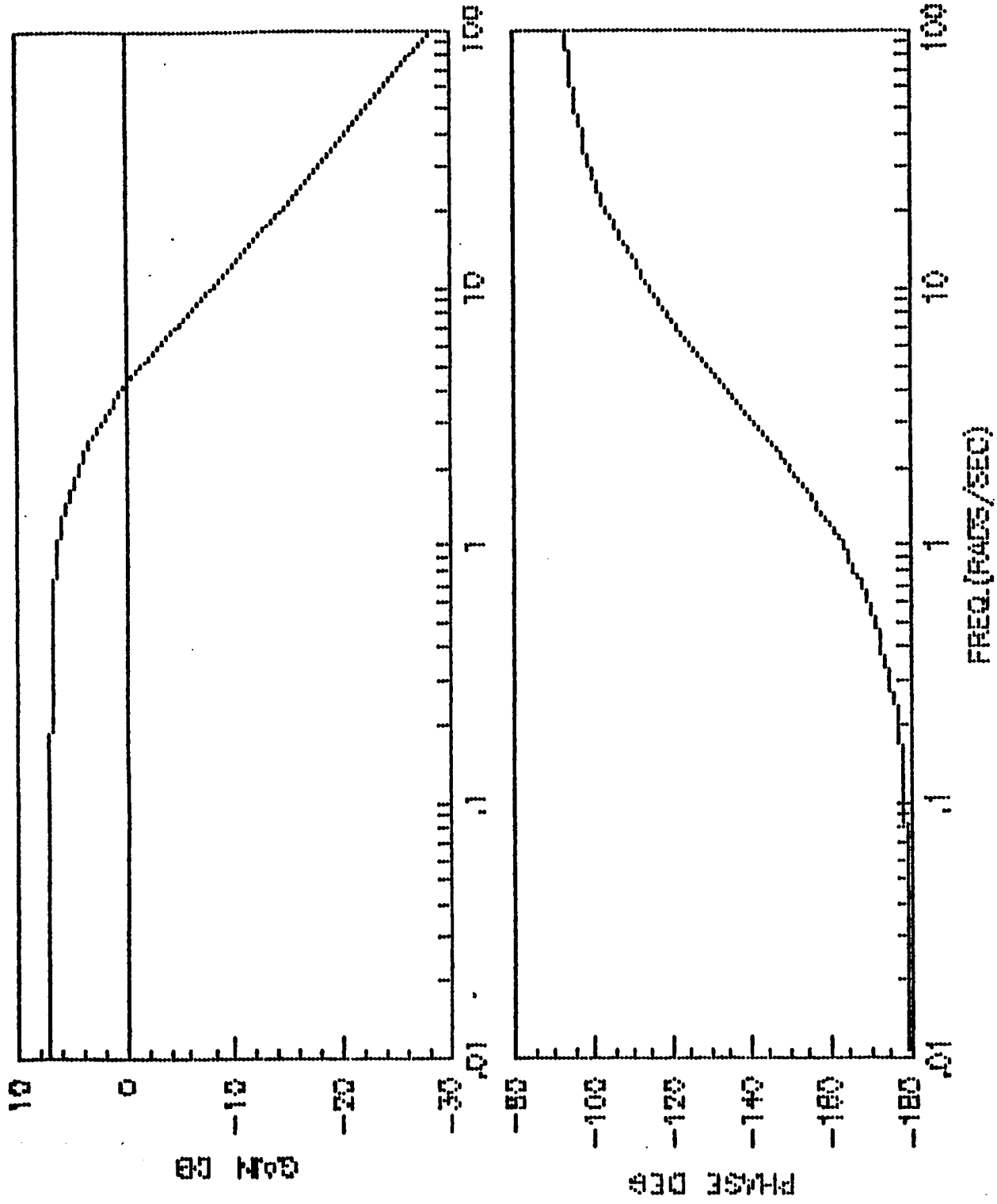

Figure 3.7(a) Bode plots for δ_H loop open

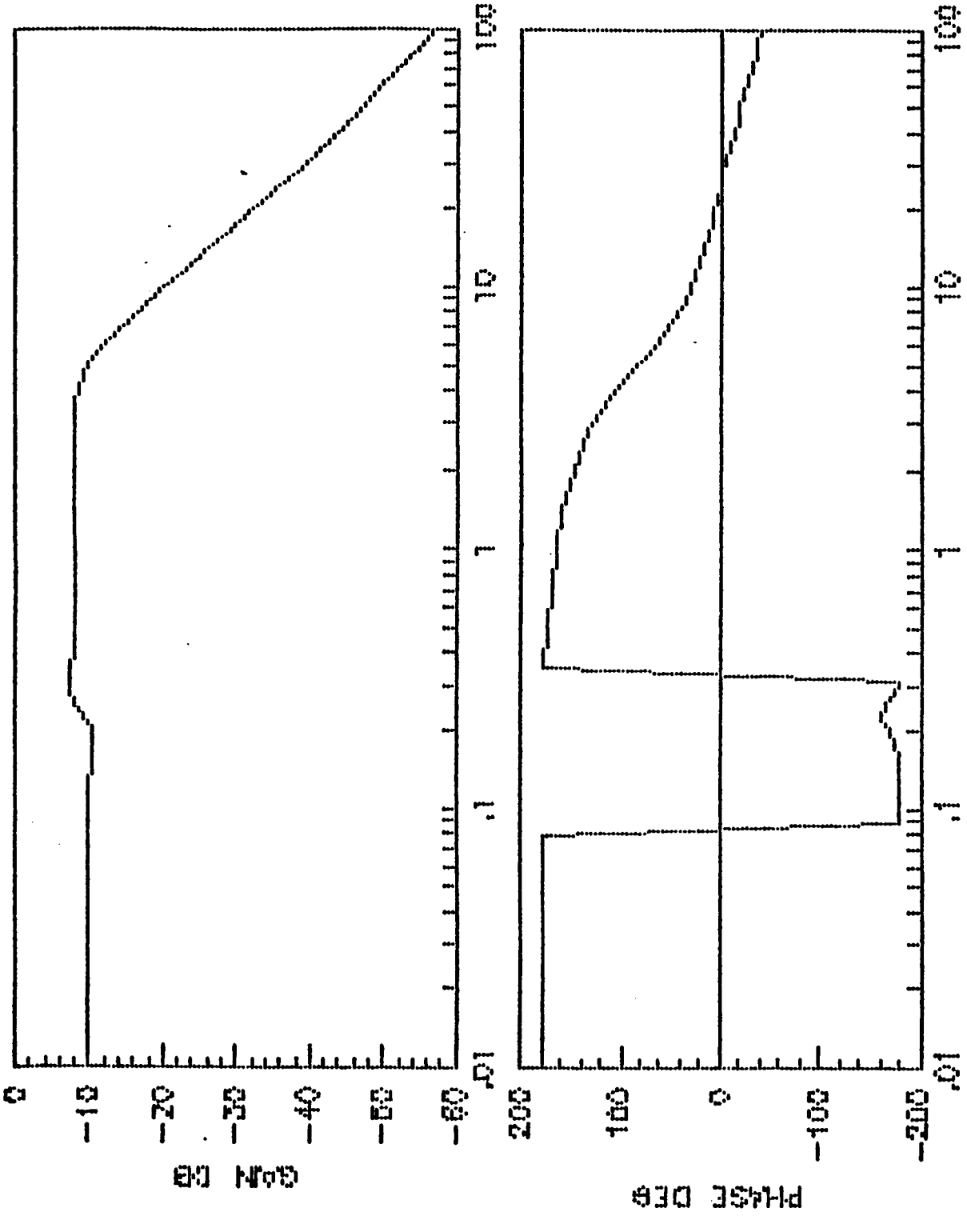

Figure 3.7(b) Bode plots for δ_{TV} loop open

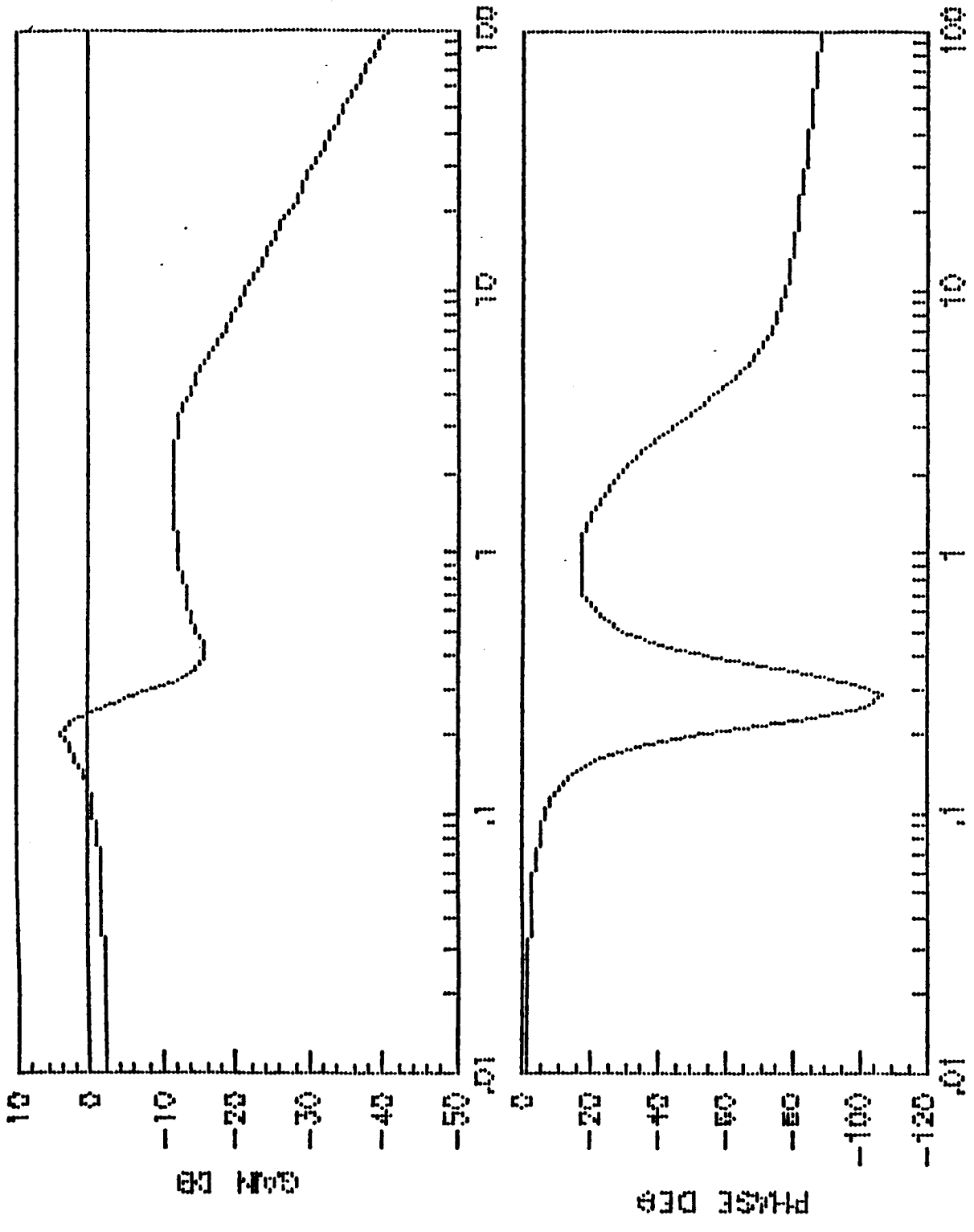

Figure 3.7(c) Bode plots for δ_F loop open

4. EXPLICIT MODEL FOLLOWING (EMF)

4.1 Gain Synthesis

In the LQ explicit model-following algorithm, the problem formulation is as follows

Given vehicle dynamics

$$\dot{\bar{x}}_v = A_v \bar{x}_v + B_v \bar{u}$$

$$\bar{z}_v = C_v \bar{x}_v$$

where $\bar{z}_v$ is the vector of vehicle responses to be controlled, and desired system characteristics in the form of a state-space model

$$\dot{\bar{x}}_m = A_m \bar{x}_m + B_m \delta_{st}$$

$$\bar{z}_m = C_m \bar{x}_m$$

where δ_{st} = pilot stick input modelled as

$$\dot{\delta}_{st} = -\frac{1}{\tau_p} \delta_{st} + \frac{1}{\tau_p} w_p \quad , \quad w_p \text{ "white" with intensity } W$$

we want to determine $\bar{u}$ to minimize

$$J_E = E\left\{ \lim_{T\to\infty} \frac{1}{T} \int_0^T \left[(z_v - z_m)^T Q_z (z_v - z_m) + u^T R u \right] dt \right\}$$

Combining the vehicle dynamics and the model dynamics, we get

$$\begin{bmatrix} \dot{\bar{x}}_v \\ \dot{\bar{x}}_m \\ \dot{\delta}_{st} \end{bmatrix} = \begin{bmatrix} A_v & 0 & 0 \\ 0 & A_m & B_m \\ 0 & 0 & -\frac{1}{\tau_p} \end{bmatrix} \begin{bmatrix} \bar{x}_v \\ \bar{x}_m \\ \delta_{st} \end{bmatrix} + \begin{bmatrix} B_v \\ 0 \\ 0 \end{bmatrix} \bar{u} + \begin{bmatrix} 0 \\ 0 \\ \frac{1}{\tau_p} \end{bmatrix} w_p$$

Writing the augmented state vector as $\bar{x}^T = [\bar{x}_v^T, \bar{x}_m^T, \delta_{st}]$ and with appropriate definitions of the matrices A, B, C and D, we can write the combined system dynamics as

$$\dot{\bar{x}} = A\bar{x} + B\bar{u} + D w_p$$

$$\bar{z}_e = z_v - z_m = C\bar{x}$$

and J_E can be written as

$$J_E = E\left\{\lim_{T\to\infty} \frac{1}{T}\int_0^T \left[\bar{x}^T C^T Q_z C \bar{x} + \bar{u}^T R \bar{u}\right] dt\right\}$$

The problem is now in the form of a Linear Quadratic Regulator (LQR) and the resulting control law is [6]

$$\bar{u} = -K\bar{x} = \begin{bmatrix} -K_V & -K_m & -K_{st} \end{bmatrix} \begin{bmatrix} \bar{x}_V \\ \bar{x}_m \\ \delta_{st} \end{bmatrix}$$

with

$$K = R^{-1} B^T P$$

and $P \geq 0$ and symmetric, the solution to the algebraic Ricatti equation

$$A^T P + PA + C^T Q_z C - PBR^{-1}B^T P = 0$$

The block diagram for EMF control law implementation is shown in Fig. 4.1. A macro using MATRIX$_X$ commands for the synthesis of the EMF control law is documented in the Appendix.

The augmented system results in the following state-space representation

$$\begin{bmatrix} \dot{\bar{x}}_V \\ \dot{\bar{x}}_m \end{bmatrix} = \begin{bmatrix} A - B_V K_V & -B_V K_m \\ 0 & A_m \end{bmatrix} \begin{bmatrix} \bar{x}_V \\ \bar{x}_m \end{bmatrix} + \begin{bmatrix} -B_V K_{st} \\ B_m \end{bmatrix} \delta_{st}$$

$$z_V = \begin{bmatrix} C_V & 0 \end{bmatrix} \begin{bmatrix} \bar{x}_V \\ \bar{x}_m \end{bmatrix}$$

3.2 Model Selection and Resulting Control Law

The vehicle state-space representation is as in Section 2.1 with all the three inputs ($\delta_{H_c}, \delta_{TV_c}, \delta_{F_c}$) and the vehicle responses to be controlled, $\bar{z}_V^T = [q, \theta, \gamma]$.

With the handling quality criteria stated in terms of desired short period response for the augmented system, we have

$$\frac{q_m}{\delta_{st}} = \frac{K_q (s + 1/\tau_{\theta_2})}{(s^2 + 2\zeta_{sp}\omega_{sp}\, s + \omega_{sp}^2)}$$

and

$$\frac{\gamma_m}{\theta_m} = \frac{K_\gamma (1/\tau_{\theta_2})}{(s + 1/\tau_{\theta_2})}$$

In the state-space form, this model can be represented as the third order system

$$\begin{bmatrix} \dot{x}_1 \\ \dot{x}_2 \\ \dot{x}_3 \end{bmatrix} = \begin{bmatrix} 0 & 1 & 0 \\ 0 & 0 & 1 \\ 0 & -\omega_{sp}^2 & -2\zeta_{sp}\omega_{sp} \end{bmatrix} \begin{bmatrix} x_1 \\ x_2 \\ x_3 \end{bmatrix} + \begin{bmatrix} 0 \\ 0 \\ 1 \end{bmatrix} \delta_{st}$$

$$\bar{z}_m = \begin{bmatrix} q_m \\ \theta_m \\ \gamma_m \end{bmatrix} = \begin{bmatrix} 0 & K_q(1/\tau_{\theta_2}) & K_q \\ K_q(1/\tau_{\theta_2}) & K_q & 0 \\ K_\gamma(1/\tau_{\theta_2})K_q & 0 & 0 \end{bmatrix} \begin{bmatrix} x_1 \\ x_2 \\ x_3 \end{bmatrix}$$

With $K_\gamma = 1$, $\omega_{sp} = 3.7$ rads/sec, $\zeta_{sp} = 0.75$, $\tau_{\theta_2} = 0.75$ sec and $K_q = 5.133$ rads/sec/rad (based on stick gradient of 1°/lb), the numerical values of the model system matrices are listed in Table 4.1

For the purposes of the following control law synthesis, the stick time constant $\tau_p = 0.1$ sec,

and the output error weighting matrix Q = I were chosen. The control weighting matrix R was chosen as

$$R = \rho \begin{bmatrix} \frac{1}{(\delta_{H_{max}})^2} & 0 & 0 \\ 0 & \frac{1}{(\delta_{TV_{max}})^2} & 0 \\ 0 & 0 & \frac{1}{(\delta_{F_{max}})^2} \end{bmatrix} = \rho \begin{bmatrix} 0.01 & 0 & 0 \\ 0 & 0.00111 & 0 \\ 0 & 0 & 0.04 \end{bmatrix}$$

where subscript "max" refers to the maximum allowable deflection. As the "control authority" is increased (scalar weighting ρ is decreased), the crossover frequency of the loop transfer functions $K_V[sI - A]^{-1}B_V$ will increase. Higher loop cross-over, in general, relates to a higher fidelity match of the vehicle and model. However, higher crossover frequency can also increase the chance of the control system exciting the unmodelled modes (i.e. structural modes) and may lead to undesirably

high control deflections. A value of $\rho = 1$ was chosen for this preliminary investigation. Although the resulting loop transfer functions are not presented here, the cross-over frequencies for the chosen value of ρ were found to be quite high. (≈ 10 rad/s)

For the above problem formulation, the feedback gains obtained by exercising the solution algorithm are listed in Table 4.2.

4.3 Performance Evaluation

For the control law synthesized as above, the transfer functions of interest for the augmented system are listed in Table 4.3. From the $\frac{q}{\delta_{st}}$ and $\frac{\gamma_{CR}}{\delta_{st}}$ transfer functions, we note that unlike the DEA case, model reduction is required in order to get the low-order equivalent system parameters to determine the handling qualities of the augmented system.

The desired frequency responses (from the model) and those for the augmented vehicle are compared in Figs. 4.2 to 4.4. Fig. 4.2 shows that the pitch rate frequency response for the vehicle closely approximates the model response for frequencies upto 10 rads/sec. Fig. 4.3 shows a fair agreement between the desired flight path angle response and that obtained at the center of rotation through augmentation. Fig. 4.4 compares the resulting flight path angle to pitch attitude relationship with that desired. This last result is quite unsatisfactory and a redesign with higher control authority may be required in order to obtain a better fit between the model and the augmented vehicle.

Time histories for a step pilot input ($\delta_{st} = 1^{\circ}$) are shown in Figs. 4.5 to 4.7. From the u, α, q and θ responses in Fig. 4.5, we note that the augmented vehicle does exhibit "classical" aircraft like dynamics. The normal acceleration and the flight path angle response, both at the

C.G. as well as the C.R., are shown in Fig. 4.6. The control deflections for a step stick input are shown in Fig. 4.7.

4.4 Robustness Evaluation

Using the block diagram of Fig. 4.1, the stability robustness of the EMF design may be evaluated by considering the values of $\underline{\sigma}[\mathcal{I} + K_V G_V(j\omega)]$, where $G_V(s) = [s\mathcal{I} - A_V]^{-1} B_V$. The singular values of this return difference matrix for the design obtained above are shown in Fig. 4.8. Note that these stability margins are better than those obtained for the DEA design. If even higher stability margins are desired, then a control redesign with an appropriate choice of the control weighting matrix R may be required.

Table 4.1 Model System Matrices

$$\bar{z}_m^T = [q_m, \theta_m, \gamma_m]$$

AM =

$$\begin{bmatrix} 0. & 1.0000 & 0. \\ 0. & 0. & 1.0000 \\ -0.0010 & -13.6900 & -5.5500 \end{bmatrix}$$

BM =

$$\begin{bmatrix} 0. \\ 0. \\ 1. \end{bmatrix}$$

CM =

$$\begin{bmatrix} 0. & 6.8440 & 5.1330 \\ 6.8440 & 5.1330 & 0. \\ 6.8440 & 0. & 0. \end{bmatrix}$$

Table 4.2 Feedback gains for EMF design

KV =

$$\begin{bmatrix} 3.7289 & -4.1093 & -3.7624 & 0.4547 & 0.2634 & 0.1986 & -0.0083 \\ -1.8472 & 5.6138 & -28.8149 & -37.3867 & 1.7893 & 1.4723 & -0.2548 \\ 0.6307 & -2.3144 & 0.2141 & 2.9170 & -0.0021 & -0.0071 & 0.0161 \end{bmatrix}$$

KM =

$$\begin{bmatrix} -22.8453 & 14.9659 & 12.8585 \\ 250.0815 & 268.2479 & 120.7149 \\ -19.7479 & -7.6633 & -1.2971 \end{bmatrix}$$

KST =

$$\begin{bmatrix} 0.4056 \\ 5.5389 \\ -0.0921 \end{bmatrix}$$

Table 4.3 Transfer Functions for EMF design

$$\Delta = s(s+2.775 \pm j\,2.4473)(s+0.908 \pm j\,0.1297)(s+0.184)(s+15)(s+15)(s+20.14 \pm j\,17.1)$$

$$\frac{q}{\delta_{st}} = \frac{130(s+0.188)(s+0.618)(s+1.226 \pm j\,0.38)(s+15)(s+15)(s+25.82)s}{\Delta}$$

$$\frac{n_z}{\delta_{st}} = \frac{-26.419(s-0.00342)(s+0.2)(s+1.088)(s+2.52 \pm j\,0.784)(s-4.801)(s+14.58)(s+15)(s+26.76)}{\Delta}$$

$$\frac{r}{\delta_{st}} = \frac{-4.428(s+0.196)(s+1.091)(s+2.484 \pm j\,0.762)(s-4.71)(s+14.58)(s+15)(s+26.76)}{\Delta}$$

$l_{CR} = 6.54$ ft ;

$$\frac{n_{z_{CR}}}{\delta_{st}} = \frac{31.764(s-0.00342)(s+0.2)(s+1.093)(s+2.357)(s+9.17)(s+10)(s+15)(s+49.5)}{\Delta}$$

$$\frac{r_{CR}}{\delta_{st}} = \frac{-0.2615(s+0.197)(s+1.097)(s+2.34)(s+6.64)(s+12.44)(s+15)(s+34.22)(s-38.14)}{\Delta}$$

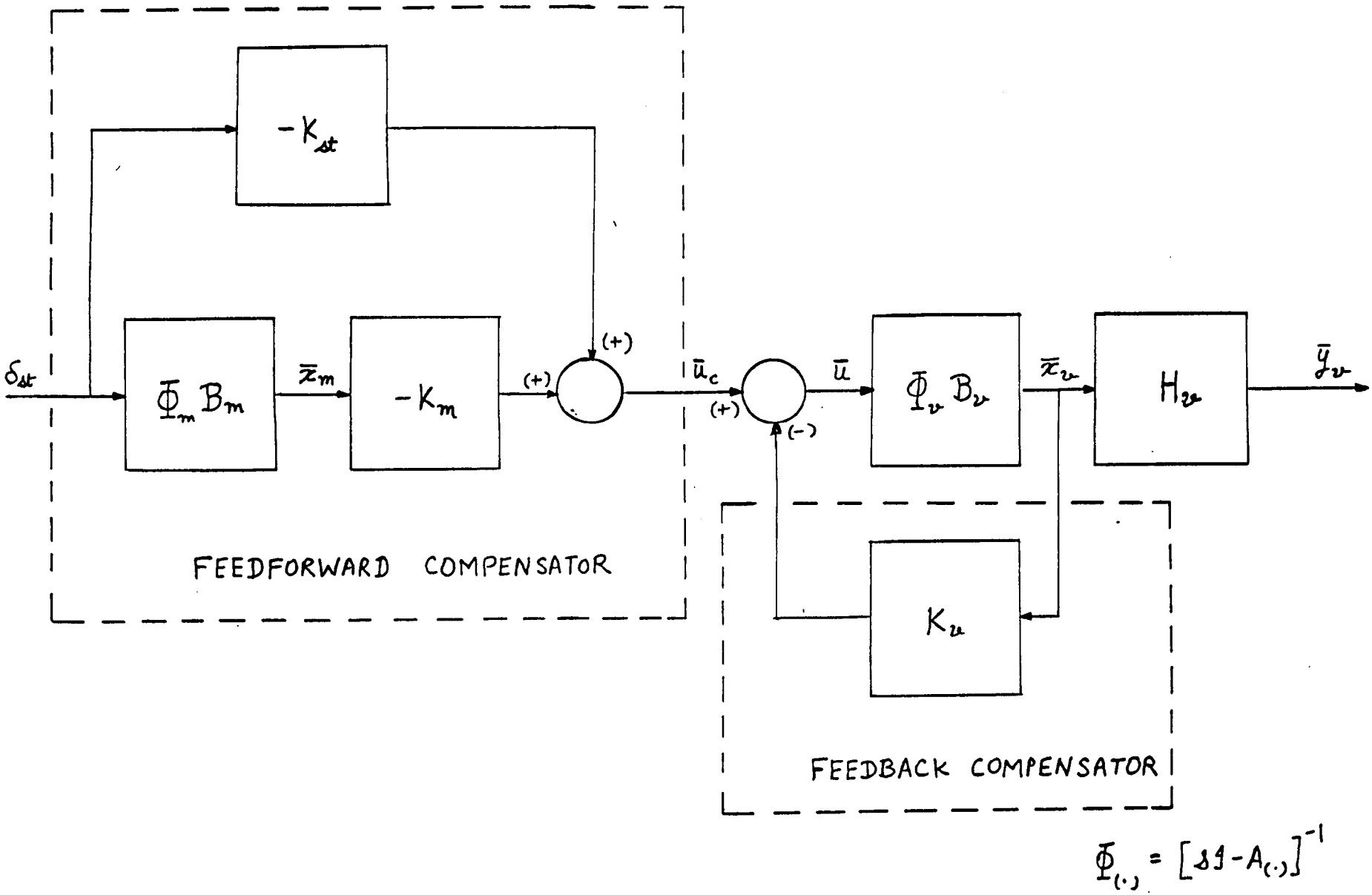

Figure 4.1 EMF Control Law Implementation

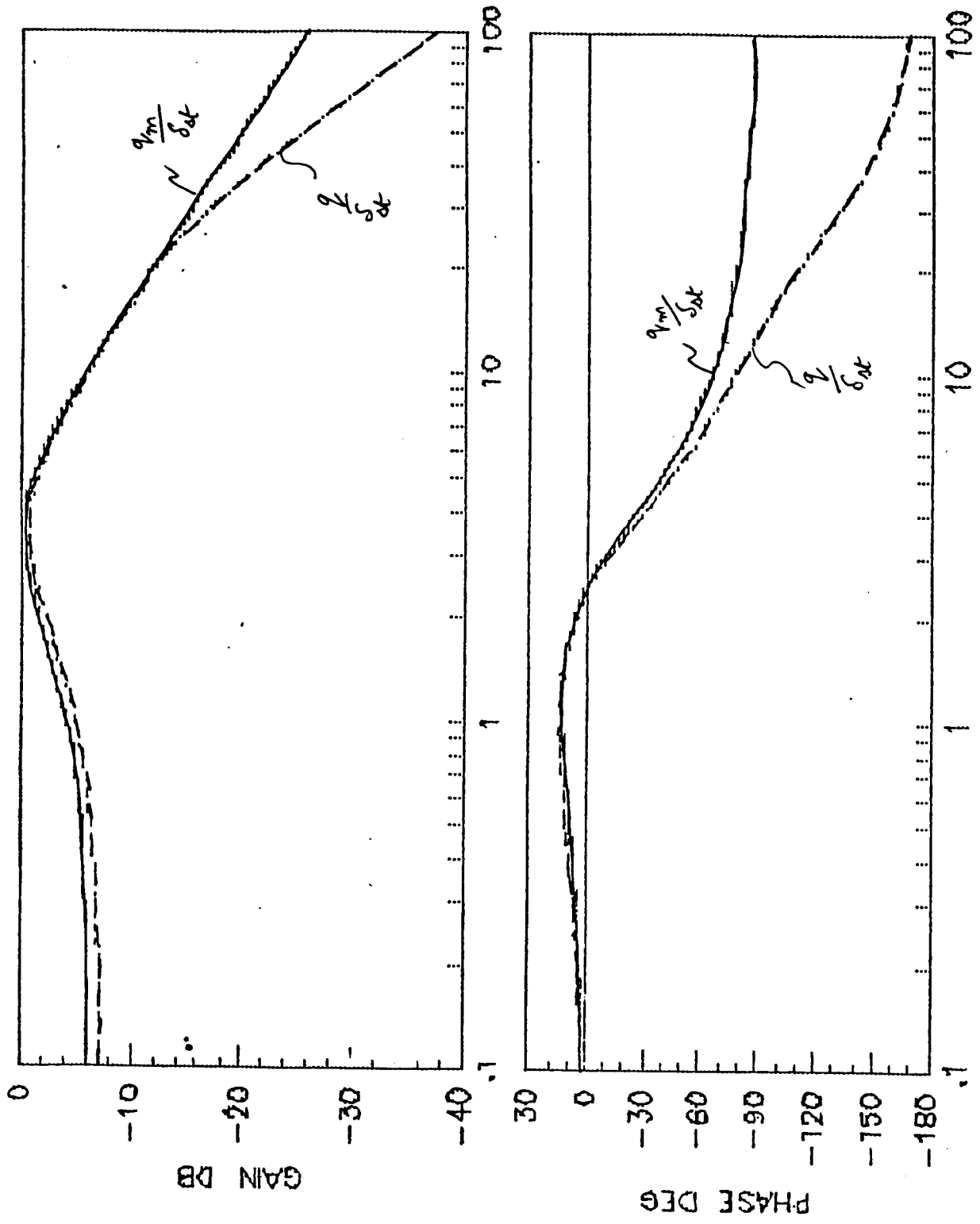

Figure 4.2 $\frac{q_m}{\delta_{st}}$ and $\frac{q}{\delta_{st}}$ for augmented vehicle

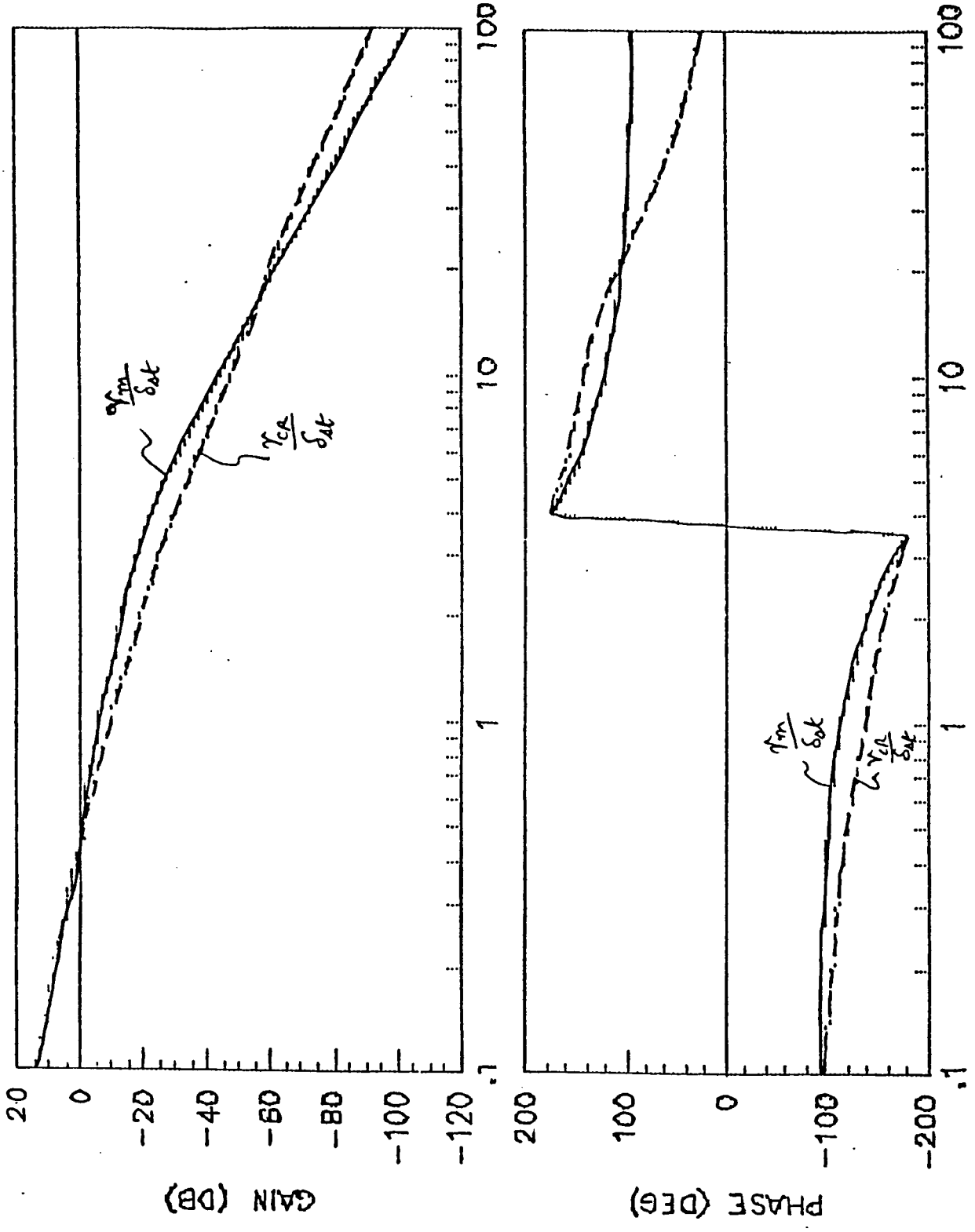

Figure 4.3 $\frac{\gamma_m}{\delta_{st}}$ and $\frac{\gamma_{cg}}{\delta_{st}}$ for augmented vehicle

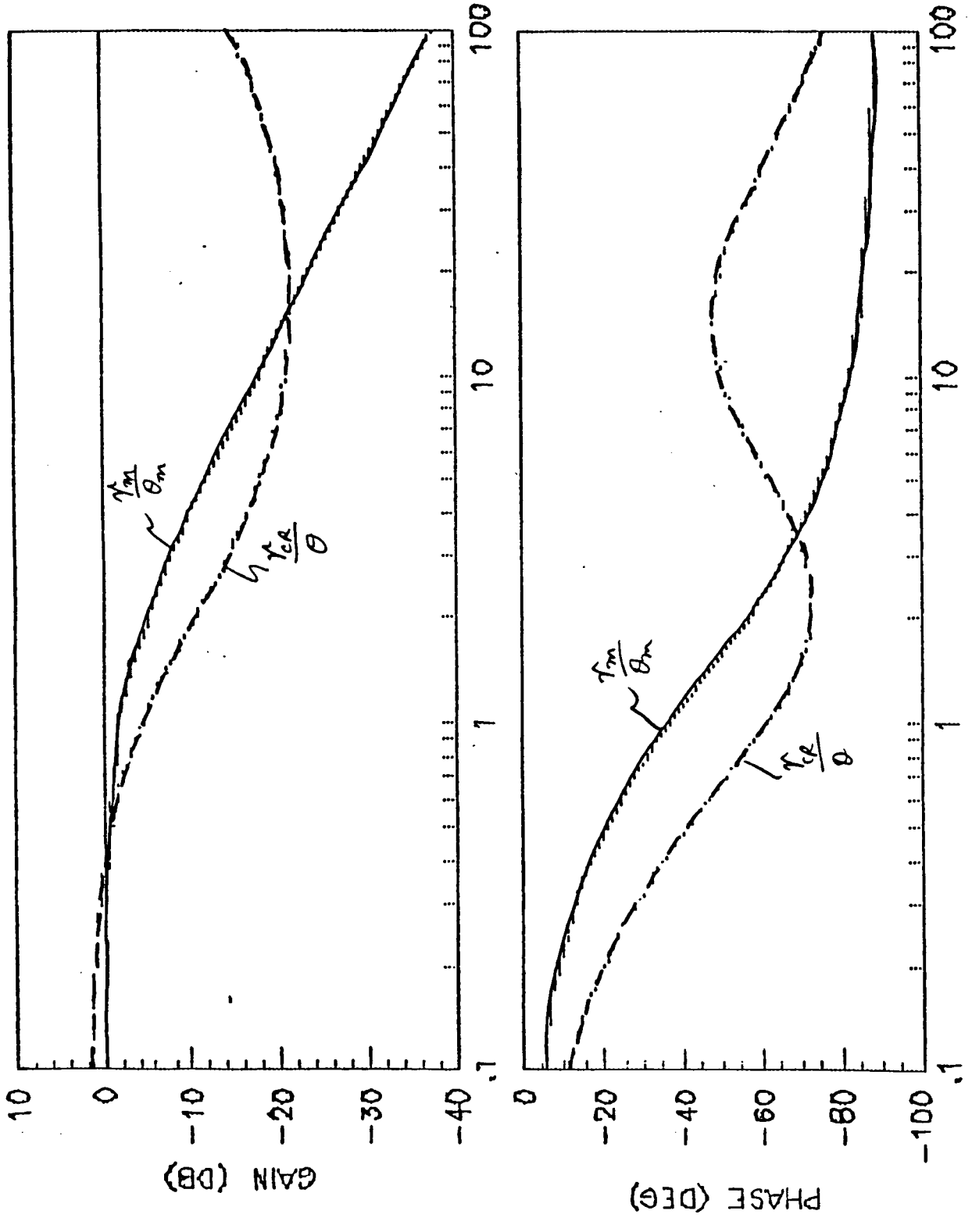

Figure 4.4 $\frac{\gamma_m}{\theta_m}$ and $\frac{\gamma_{cR}}{\theta}$ for augmented vehicle

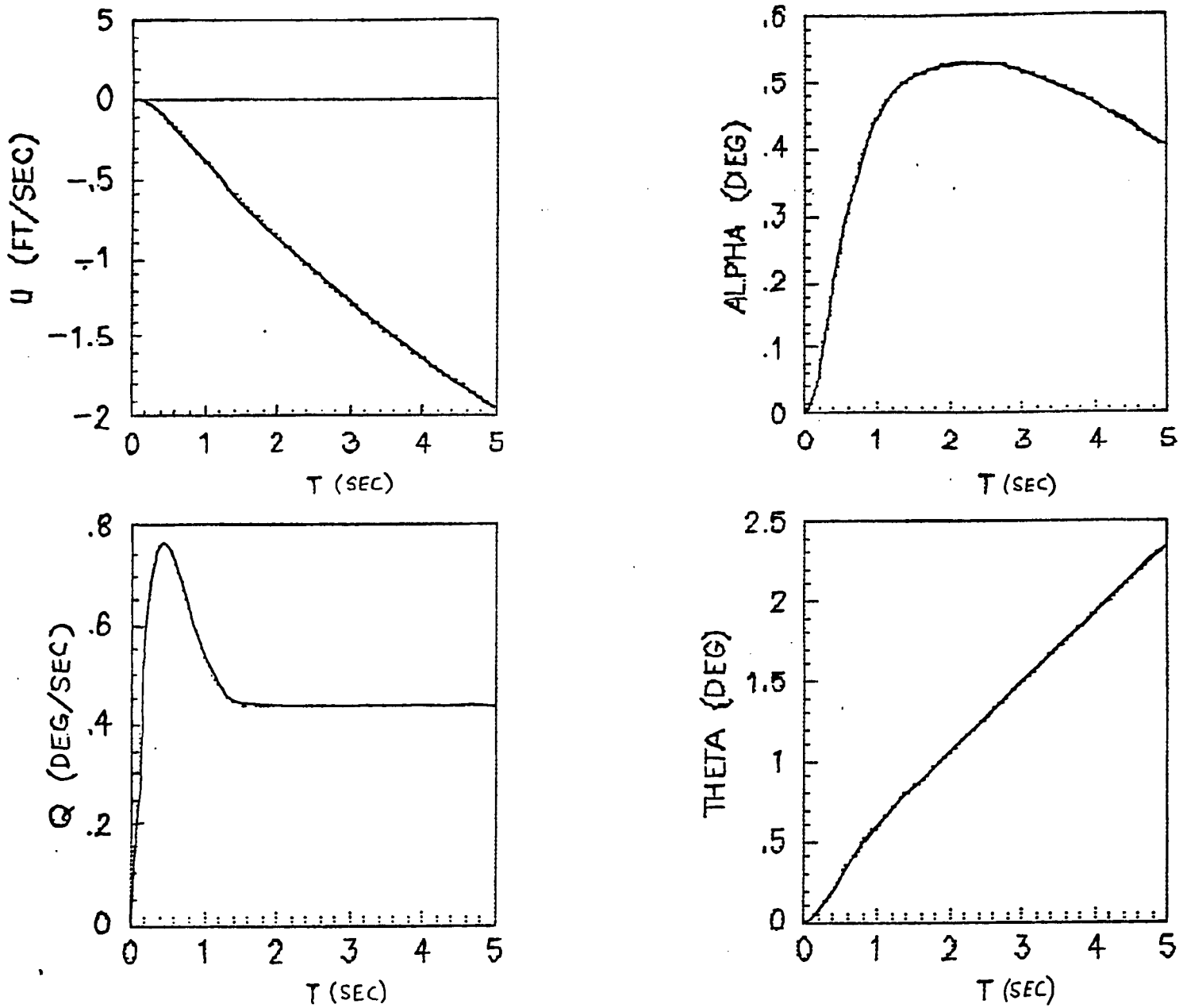

Figure 4.5 Augmented vehicle response for step pilot input ($\delta_{si} = 1°$)

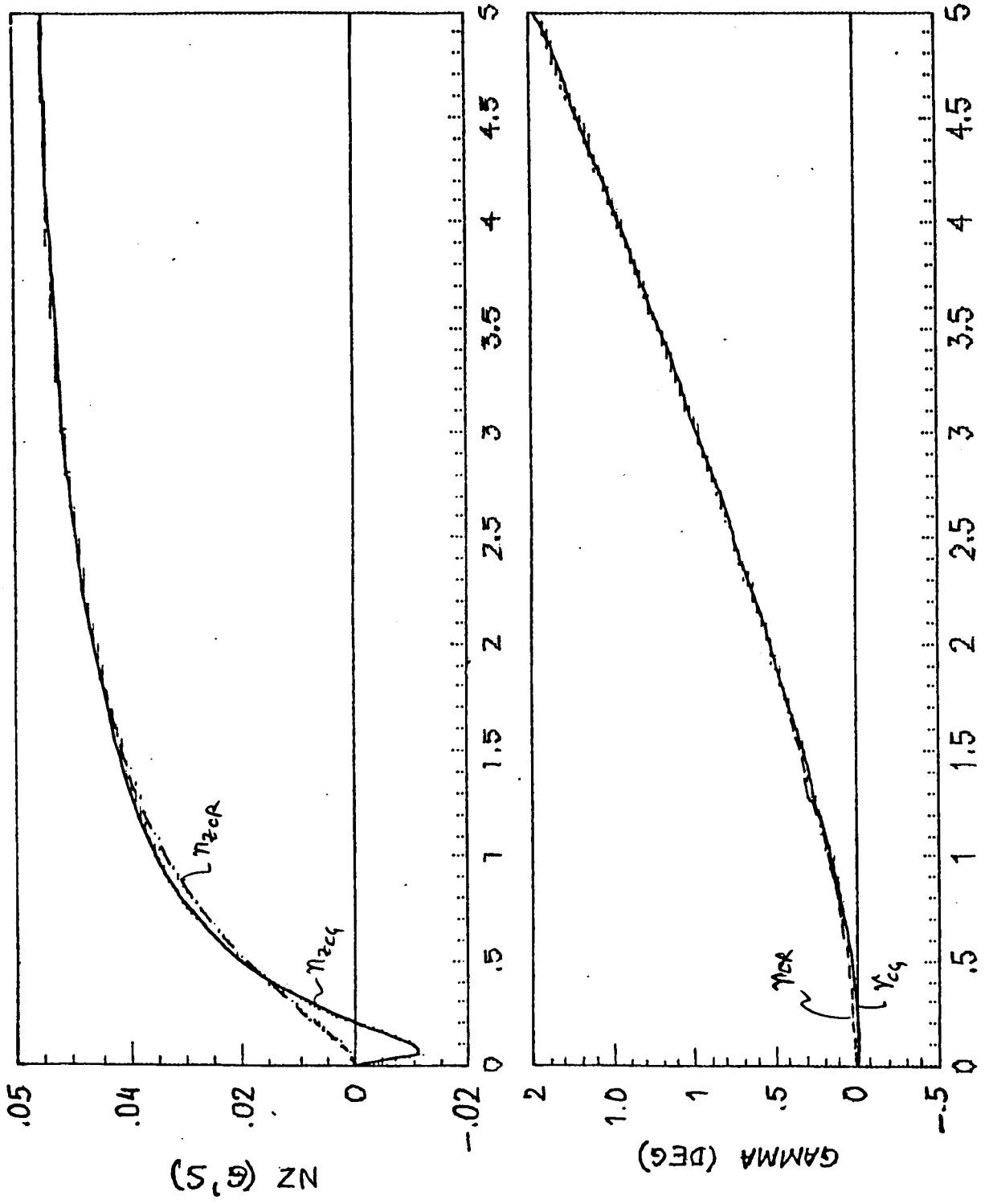

Figure 4.6 n_z and γ response for step pilot input (δ_{st}=1°)

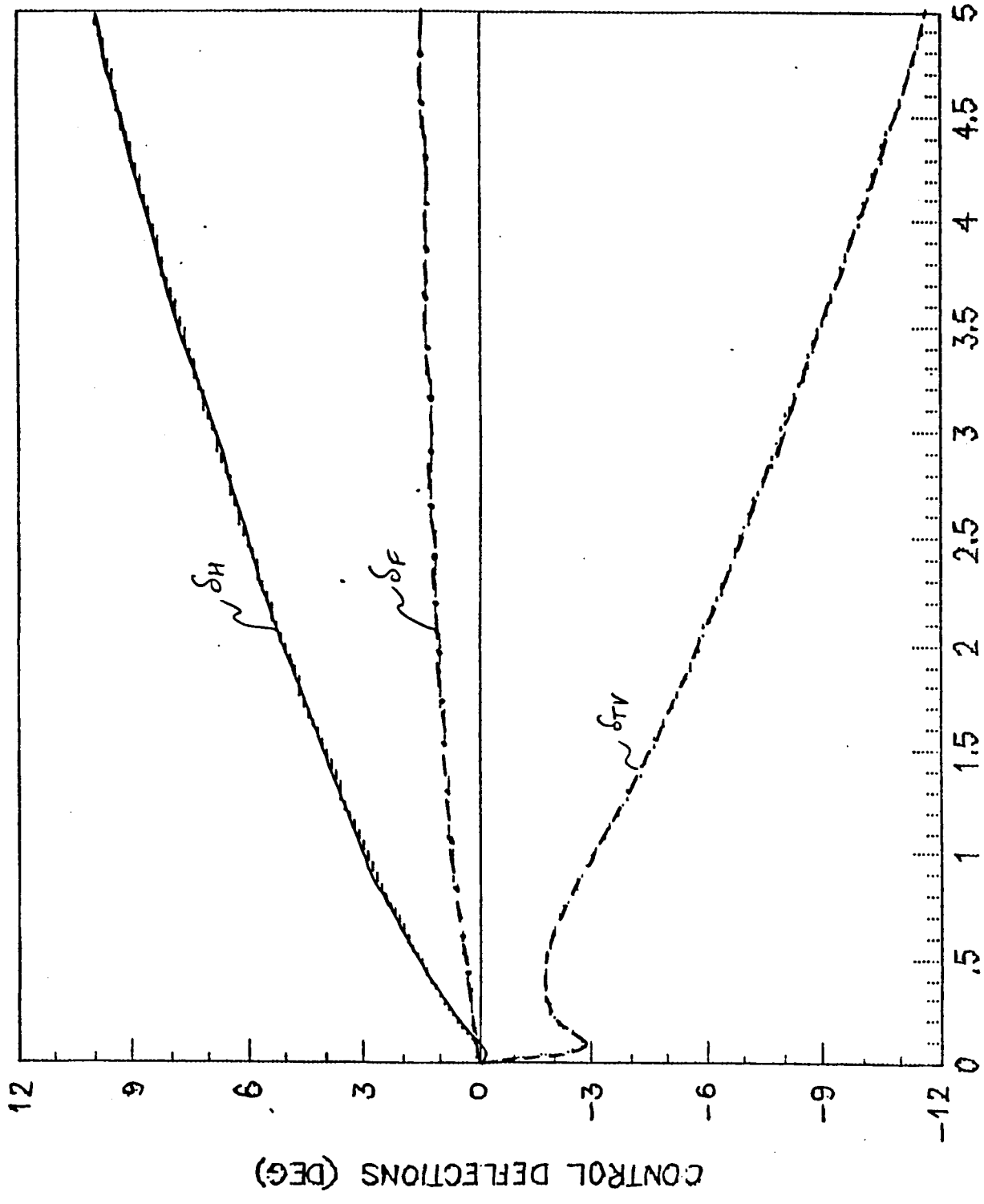

Figure 4.7 Control Deflections for step pilot input (δ_{st}=1°)

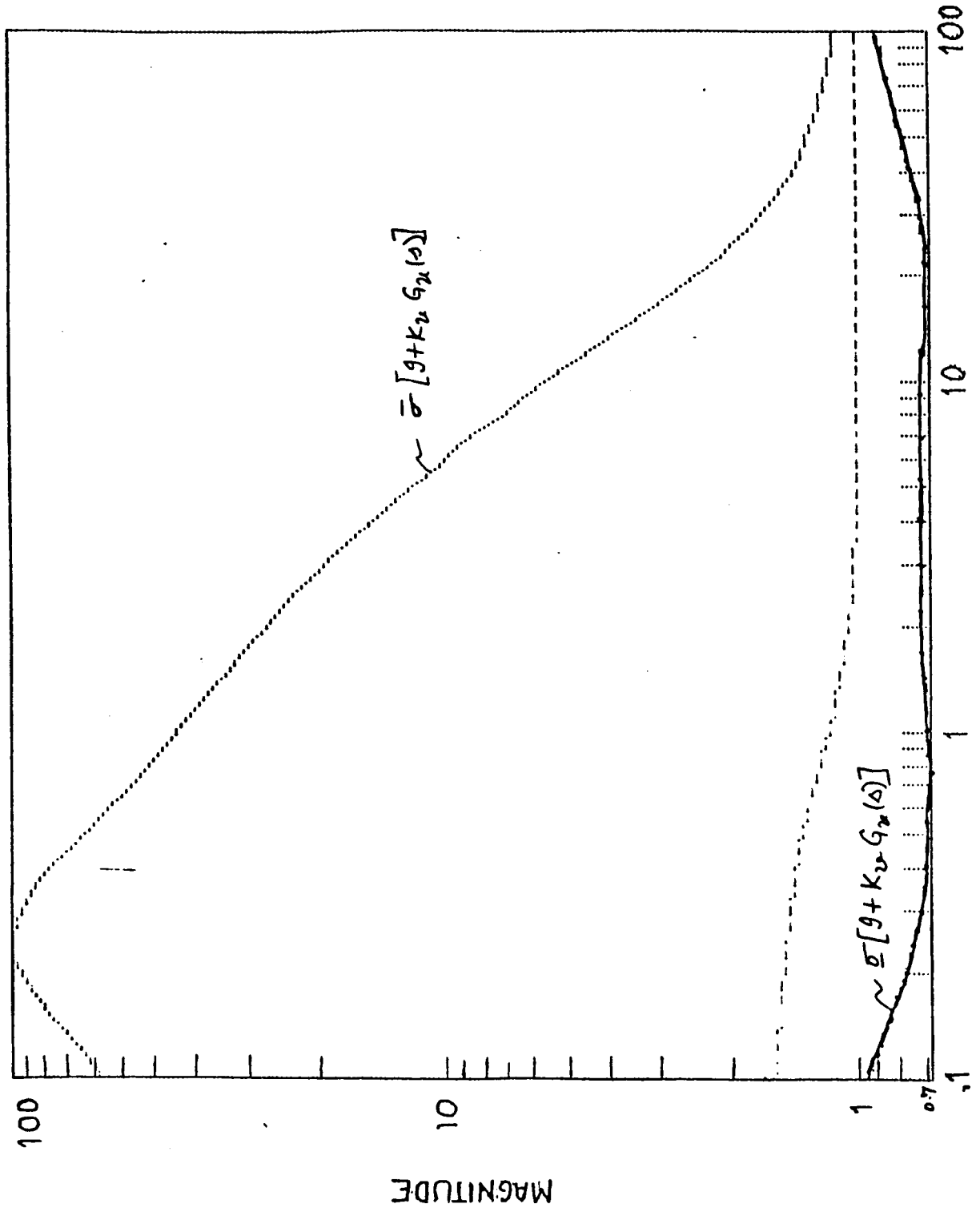

Figure 4.8 Singular values of return difference matrix at input (EMF design)

5. IMPLEMENTATION USING OUTPUT FEEDBACK

Both the synthesis algorithms discussed herein lead to state feedback control laws. Since in practice, not all the states of a system are measurable, an estimator design is required. Two issues that arise with estimation are the effect on transient response and robustness. Two methods, which can be used to implement the full-state control laws, that are worthy of consideration and will be pursued further in the future, are cited here.

5.1 Robust Kalman Filter

This procedure is as discussed in [7,8] and consists of parametrically increasing the process noise in the Kalman filter synthesis procedure till the full-state loop robustness is recovered. Properly implemented, this procedure does not increase the dynamic order of the stick-response transfer functions.

5.2 Robust Output Observers

This procedure is as discussed in [9] and consists of using observer theory to reconstruct system states from the available measurments. The advantages of this approach are that it leads to low order and guaranteed stable controllers and the state-feedback system is fully reconstructed so there is no deterioration in performance and robustness. The procedure takes advantage of certain system structure, and therefore cannot always be applied, however.

6. Conclusions

Some important conclusions based on the design examples addressed to date are as follows

DEA

The direct eigenspace assignment technique has the advantage that the resulting augmented system is of the same dynamic order as the open-loop system, which means that once the design is performed, the handling qualities evaluation of the augmented system can directly be carried out. Also, once the design requirements are properly mapped into the form of a desired eigenstructure, the solution algorithm for obtaining the "closest possible" eigenstructure for the augmented system is quite straightforward.

Some of the areas that require further investigation to make the DEA design technique more viable are

a. Procedures for selecting the desired eigennstructure such that the choice reflects the control system design objectives.

b. Procedures for improving the stability robustness of the feedback design

c. Prefilter design to properly blend the control inputs such that the desired dynamics are obtained from the pilot's stick input.

EMF

Though the EMF technique has the advantage that the flight control design requirements are easily mapped into the design pro-

cedure, its major disadvantages are that the resulting augmented system is of high order and the required bandwidth may be high. This means that system reduction is required in order to evaluate the handling qualities of the augmented system. This needs to be done for the control law synthesized herein. Finally, very high bandwidth control laws may be susceptible to model errors and require high deflection rates.

REFERENCES

[1] Anon., Military Specification - Flying Qualities of Piloted Airplanes, MIL-F-8785C, USAF, Wright Patterson AFB, Ohio, 1980.

[2] Schmidt, David K., and Davidson, John B., "Flight Control Law Synthesis for an Elastic Vehicle by Eigenspace Assignment", AIAA paper 85-1898, AIAA Guidance, Navigation and Control Conference, Snowmass, Colorado, August 1985.

[3] Davidson, John B., "Flight Control Synthesis of Flexible Aircraft using Eigenspace Assignment", M.S. Thesis, Purdue University, West Lafayette, Indiana, May 1985.

[4] Andry, A.N., Shapiro, E.Y., and Chung, J.C., "On Eigenstructure Assignment for Linear Systems", IEEE Trans. on Aerospace and Electronic Systems, Vol. AES-19, No. 5, September 1983.

[5] Lehtomaki, N.A., Sandell, N.S., Jr., and Athans, M., "Robustness results in Linear Quadratic Gaussian based Multivariable Control Designs", IEEE Trans. on Automatic Control, Vol. 26, Feb. 1981, pp. 75-92.

[6] Kwakernaak, H., and Sivan, R., "Linear Optimal Control Systems", Wiley-Interscience, 1972.

[7] Doyle, J.C., Stein, G., "Robustness with Observers", IEEE Trans. on Automatic Control, Vol. AC-24, No. 4, August 1979.

[8] Schmidt, David K., and Foxgrover, John A., "Multivariable Control Synthesis Approaches to Meet Handling Qualities Objectives", AIAA Paper No. 84-1831, AIAA Guidance and Control Conference, Seattle, Washington, August 1985.

[9] Rynaski, E.G., "Flight Control System Design using Robust Output Observers", AGARD CP321, "Advances in Guidance and Control Systems", Lisbon, Portugal, Oct. 1982.

APPENDIX

The macro for direct eigenspace assignment is listed in Table A.1 and that for explicit model following in Table A.2. Both the macros are written in the form of "user defined functions" and can be executed inside MATRIX$_X$. Also, the macros are well documented with comment cards so that the user can understand the input-output requirements.

Table A.1 Macro 'eigassgn' for DEA design

```
// [va,fbkr]=eigassgn(a,b,nc,nsp,lamcl,vd,qd)
// state feedback gains for eigenspace assignment
// inputs are a, b, nc, nsp, lamcl, vd, qd
// a - system matrix
// b - system control distribution matrix
// nc - no. of desired complex poles / 2
// nsp - no. of complex poles for which the weighting on the eigenvector
//       error is different for real and imaginary parts
// lamcl - column vector of desired closed loop poles with nc+nr elements
//         where nr is the no. of desired real poles
//         first nc elements are the desired complex poles with +ve imag. part
//         with the nsp elements appearing first
// vd - n by (nc+nr) matrix of desired eigenvectors with ith column corr. to
//      ith element of lamcl
// qd - n by (nsp+nc+nr) matrix of weigthing on eigenvector errors; ith column
//      forms the diagonal elements of the weigthing matrix of ith eigenvector
//      the first 2*nsp columns correspond to the nsp eigenvectors with
//      weighting on the real and imaginary parts appearing consecutively
//      (the real part first)
// outputs are; va, fbkr
// va - matrix of acheivable eigenvectors
// fbkr - feedback gain matrix (corr. to neg. feedback)
//
[temp1,temp2]=size(lamcl); nr=temp1-nc;
ns=2*nc+nr;
//
if nsp>0, [ns,nu]=size(b); bb=[b 0*ones(ns,nu); 0*ones(ns,nu) b];...
for i=1:nsp; j=2*i-1; qtmp=diag([qd(:,j);qd(:,j+1)]);...
vtmp=[real(vd(:,i));imag(vd(:,i))]; tmp1=real(lamcl(i))*eye(ns)-a;...
tmp2=imag(lamcl(i))*eye(ns); mtmp=[tmp1 -tmp2;tmp2 tmp1]; ...
tmp=vtmp'*qtmp*inv(mtmp)*bb*inv(bb'*inv(mtmp)'*qtmp*inv(mtmp)*bb);...
vtmp=inv(mtmp)*bb*tmp'; tmp=tmp'; w(:,j)=tmp(1:nu)+jay*tmp(nu+1:2*nu); ...
w(:,j+1)=conj(w(:,j)); va(:,j)=vtmp(1:ns)+jay*vtmp(ns+1:2*ns); ...
va(:,j+1)=conj(va(:,j));...
if i=nsp, clear qtmp bb tmp tmp1 tmp2 mtmp vtmp nu;
//
tmp1=nc-nsp;
if tmp1>0, for i=nsp+1:nc; j=2*i-1; li=inv(lamcl(i)*eye(ns)-a)*b; ...
tmp=vd(:,i)'*diag(qd(:,nsp+i))*li*inv(li'*diag(qd(:,nsp+i))*li);...
w(:,j)=tmp'; w(:,j+1)=conj(w(:,j)); va(:,j)=li*w(:,j); va(:,j+1)=conj(va(:,j))
if nr>0, for i=1:nr; j=2*nc+i; l=nc+i; li=inv(lamcl(l)*eye(ns)-a)*b; ...
tmp=vd(:,l)'*diag(qd(:,nsp+l))*li*inv(li'*diag(qd(:,nsp+l))*li); ...
w(:,j)=tmp'; va(:,j)=li*w(:,j);
//
fbk=-w*inv(va); fbkr=real(fbk);
retf
```

Table A.2 Macro 'fcemf' for LMF design

```
//[eval,kr,saug,num]=fcemf(sv,sm,tp,qez,r,hv)
// flight control explicit model following algorithm
// inputs are sv, sm, tp, qez, r, hv
// sv - vehicle system; = [av bv; cv 0]
// sm - model system; = [am bm; cm 0]
// tp - pilot stick time constant
// qez - weighting matrix for error between vehicle and model outputs
// r - control weighting matrix
// hv - matrix of vehicle outputs for which transfer functions are desired
// outputs are eval, kr, num
// eval - closed loop eigenvalues
// kr - state feedback gains corr. to neg. feedback
// saug - augmented system; pilot stick as input and augmnetd vehicle outputs
// num - numerator coeff. of augmented vehicle output transfer functionss
//       (ith row corr. to ith output)
//
[ny,nv]=size(hv);
[t1,t2]=size(sv);nu=t2-nv;nz=t1-nv;[t3,nm1]=size(sm);nm=nm1-1;
a=[sv(1:nv,1:nv) 0*ones(nv,nm1); 0*ones(nm,nv) sm(1:nm,1:nm1);
0*ones(1,nv+nm), -1/tp]; b=[sv(1:nv,(nv+1):t2); 0*ones(nm1,nu)];
c=[sv((nv+1):t1,1:nv), -sm(nm1:t3,1:nm) 0*ones(nz,1)];
q=c'*qez*c;
//
[eval,kr]=regulator(a,b,q,r);
temp=a-b*kr;eval=eig(temp);
//
t4=nm+nv;
aaug=temp(1:t4,1:t4);baug=temp(1:t4,t4+1);
caug=[hv 0*ones(ny,nm)];saug=[aaug baug;caug 0*ones(ny,1)];
[num,den]=tform(saug,t4);
retf
```